Journal of
Mechanics of
Materials and Structures

ON THE VIBRATION SIMULATION OF SUBMERGED PIPES:
STRUCTURAL HEALTH MONITORING ASPECTS

Pejman Razi and Farid Taheri

msp

ON THE VIBRATION SIMULATION OF SUBMERGED PIPES: STRUCTURAL HEALTH MONITORING ASPECTS

PEJMAN RAZI AND FARID TAHERI

This work aims to provide further insight into the modeling aspects and influence of some important parameters involved in the simulation of vibration of submerged pipes, especially in relation to vibration-based structural health monitoring (VB-SHM) techniques. Two widely used techniques for modeling submerged pipelines, namely the "added mass" and "coupled acoustic-structural" approaches are compared, and their limitations and advantages in the context of VB-SHM are highlighted. Moreover, the paper also presents a comprehensive study of the effect of operational variability on the accuracy of VB-SHM of offshore pipelines. It is demonstrated that the geometric stiffness produced by the operational variability (such as changes in the internal and external pressures of pipelines) could variably alter the overall stiffness of such submerged bodies, hence affecting their dynamic response. Depending on the pipe stiffness, the imposed variations could significantly affect the accuracy of VB-SHM trials.

A list of symbols can be found on page 121.

Introduction

Vibration-based structural health monitoring (VB-SHM) of submerged structures has received several researchers' attentions in recent years [Peng and Hao 2012; Peng et al. 2012; Zhu et al. 2008; Chen et al. 2010; Na and Kundu 2002; Bao et al. 2013; Rizzo et al. 2010]. Some of these studies have included numerical simulations of their damage detection case studies in addition to their experimental verifications [Peng and Hao 2012; Peng et al. 2012; Zhu et al. 2008; Chen et al. 2010; Bao et al. 2013]. In some of those numerical studies, the fluid-structure interaction (FSI) has been idealized by using the concept of "added mass" [Peng and Hao 2012; Peng et al. 2012; Zhu et al. 2008; Bao et al. 2013] while others have adopted a more elaborate approach, namely the "coupled acoustic-structural" method, in their numerical simulations [Chen et al. 2010].

It has been shown that the idealization in representing the FSI could lead to erroneous predictions. For instance, Zeinoddini et al. [2012] compared the performances of the added mass approach (AMA) against the "coupled acoustic-structural" approach (CASA) in predicting the seismic and harmonic responses of an offshore pipeline's free-spanning (a segment of a pipe that is suspended and does not have the seabed support). They showed that the conventional AMA generally provided more conservative predictions in comparison to the CASA. With the application of the AMA, the maximum mid-span deflection of the pipe was predicted to be about 6% higher than the one obtained through the CASA. The reason was postulated to be because that the AMA inherently overlooks the dynamic pressure wave travel and therefore provides more conservative predictions.

Moreover, the simple "added mass" term can only be formulated where the velocity potential function around a vibrating structure is mathematically definable [Blevins 2001]. Kramer et al. [2013] adopted the "added-mass" term, which was originally formulated for analyzing the vibration of a submerged beam, to study the free vibration of submerged composite plates. They showed that the adoption of the AMA instead of CASA could yield inaccurate results in predicting the eigenvalues of the submerged plates with low aspect ratios (length/width). However, the predictions were in good agreement when the plates had larger aspect ratios (close to a beam-type geometry).

Therefore, in order to do an effective and accurate VB-SHM of submerged structures, one needs to gain a better understanding of the influence of such idealization in representing the associated FSI.

In addition to the modeling aspects, certain combinations of operational variables could adversely affect VB-SHM of submerged structures. Specific to offshore pipelines, variation in the internal pressure (due to a drop and/or an increase in the internal fluid's pressure) or in the external pressure (upon possible changes in the depth of submergence) could variably modify the geometric stiffness of the pipes, thereby affecting their vibration. If deviance in the vibration characteristic is noticeable, it could lead to a false alarm in detecting damage. Therefore, the VB-SHM of submerged structures would be vulnerable to the presence of such operational variability.

Zou et al. [2005] reported negligible variation in the bending eigenvalues of a composite pipe subjected to a variable internal pressure. Ross et al. [2007], however, observed significant reductions in the eigenvalues of a submerged urethane prolate when subjected to a variable external pressure.

Moreover, to the best of authors' knowledge, the influence of such operational variability on the accuracy of VB-SHM has not been addressed [Peng and Hao 2012; Peng et al. 2012; Zhu et al. 2008; Bao et al. 2013; 2011; Rezaei and Taheri 2010; Razi et al. 2013].

The present study aims to investigate the effect of above-mentioned influential parameters on the accuracy of a vibration-based damage detection methodology when applied to submerged pipes. Accordingly, the main objectives of the current research can be listed as follows.

- To identify the more suitable approach (i.e., AMA or CASA) for numerical simulation of submerged structures with particular emphasis on VB-SHM. This is achieved by comparing the efficiency and accuracy of the "added mass" and "coupled acoustic-structural" approaches in analyzing the vibration response of a submerged steel pipe.

- To gain an insight on the influence of operational variability on the accuracy of VB-SHM of submerged structures. This is addressed by investigating the vibration response of submerged steel and composite pipes that are subject to variable internal and/or external pressures.

Evaluation of the performance of "added mass" and "coupled acoustic-structural" approaches within the context of VB-SHM

In this section, the theories of AMA and CASA are first reviewed. Then the response of a submerged API-5L X65 steel pipe is numerically modeled by the two approaches, and its eigenvalues are investigated.

Theory of the added mass approach. Consider a pipe vibrating in a body of water in the direction shown in Figure 1. The dynamic response of the pipe can be determined once the applied force acting on its surface is formulated. For this purpose, the pressure distribution around the pipe's circumference
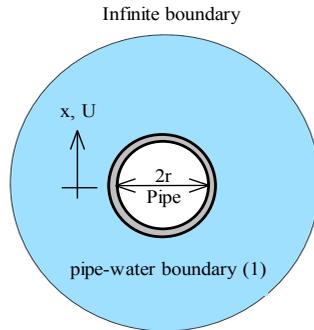
Figure 1. A pipe vibrating in a large body of fluid.

should be identified. Euler's equation [Cengel and Cimbala 2006] describes the relationship between the pressure gradient and velocity of the fluid in an unsteady flow (note that the lateral vibration of the pipe causes an unsteady flow around the pipe). For an incompressible fluid, Euler's equation can be written as

$$\frac{\partial V}{\partial t} + (V \cdot \nabla)V = -\frac{1}{\rho}\nabla p - g\nabla z. \tag{1}$$

The above equation can be simplified as [Blevins 2001]

$$\nabla\left(\frac{\partial \phi}{\partial t} + \tfrac{1}{2}V^2 + \frac{p}{\rho_f} + gz\right) = 0. \tag{2}$$

The above identity implies that the quantity within the parentheses is not a function of space. Therefore, for an arbitrary location within the fluid domain, one can assume

$$p_s = -\rho_f \frac{\partial \phi}{\partial t} - \tfrac{1}{2}\rho_f V^2 - \rho_f gh. \tag{3}$$

The above equation, which describes the static pressure as a function of the velocity potential, is called the generalized Bernoulli equation.

Bernoulli's equation is applicable to incompressible fluids and in parts of a flow in which the effect of viscosity is negligible [Cengel and Cimbala 2006]. As can be seen from (3), in order to obtain the static pressure, the velocity potential has to be identified. Once that is done, the velocity vector can be subsequently evaluated by the following equation and its magnitude substituted in (3) [Cengel and Cimbala 2006]:

$$V = \nabla\phi. \tag{4}$$

It has been shown that the velocity potential for a region around a cylinder vibrating laterally in a reservoir containing stationary fluid can be expressed by [Blevins 2001]

$$\phi = \frac{U(t)r^2[x - X(t)]}{[x - X(t)]^2 + y^2}, \tag{5}$$

where x and y are the coordinates of points of interest.

Substituting the time derivative of (5) into (3), then integrating the pressure term over the circumference of the pipe, one would obtain the net force per unit length as

$$F = -\rho_f \pi r^2 \frac{dU(t)}{dt} \boldsymbol{i}, \tag{6}$$

where $\boldsymbol{i}$ signifies the direction of the vector (here along the x axis, as shown in Figure 1). As can be seen, the force exerted by the fluid is opposing the pipe's motion since it is acting against the pipe's vibration.

It is very important to note that the term $\rho_f g h$, which represents the hydrostatic pressure in (3), has no contribution to the net force. The hydrostatic pressure is assumed to be uniformly distributed around the pipe's circumference; thus, from the perspective of total net force, the total finite forces generated by this term would cancel one another. However, this pressure could shift the eigenvalues of the pipe as will be explained in the following sections.

Assuming the motion of the pipe (cylinder) is a single-degree-of-freedom system, one can rearrange the equation of motion as

$$(M + \rho_f \pi r^2) \frac{d^2 X(t)}{dt^2} + K X(t) = 0. \tag{7}$$

In essence, the surrounding fluid imposes some extra mass onto the structure, or equivalently, the cylinder imparts part of its acceleration to the surrounding medium. The term, $\rho_f \pi r^2$ is therefore referred to as the "added mass". Note that no structural damping is considered in (7).

Coupled acoustic-structural analysis. Free vibration of a pipe in an acoustic medium can be solved numerically by the standard Galerkin discretization approach applied to the weak form of the fluid equation [Zienkiewicz et al. 2005]. The weak form representing the dynamics of the acoustic medium can be written as

$$d\Pi_f = \int_{\Omega_f} dp \left[\frac{1}{c^2} \ddot{p} - \nabla^2 p \right] d\Omega. \tag{8}$$

Equation (8) expands to the following equation once the appropriate boundary conditions specific to vibration of a pipe in an infinite acoustic medium are applied:

$$\int_{\Omega_f} \left[\delta p \frac{1}{c^2} \ddot{p} - (\nabla \delta p)^T (\nabla p) \right] d\Omega + \int_{\Gamma_1} \delta p \rho_f n^T \ddot{u} \, d\Gamma + \int_{\Gamma_2} \delta p \frac{1}{c} \dot{p} \Gamma. \tag{9}$$

The reader is referred to [Zienkiewicz et al. 2005] for derivation of the boundary conditions at the interface of solid-fluid (the second term) and the radiation boundary representing an infinite acoustic medium (the third term). In a similar manner, the weak form representing the pipe's response can be established.

To solve the above equations for a discrete domain, the displacement and the nodal acoustic pressure are approximated by

$$\begin{aligned} u &= N_u \tilde{u}, \\ p &= N_p \tilde{p}. \end{aligned} \tag{10}$$

The discrete form of the structural and acoustic domains can be represented as

$$M\ddot{\tilde{u}} + C\dot{\tilde{u}} + K\tilde{u} - Q\tilde{p} + F = 0 \tag{11}$$

and

$$S \ddot{\tilde{p}} + \widetilde{C} \dot{\tilde{p}} + H \tilde{p} + \rho_f Q^T \ddot{\tilde{u}} = 0, \tag{12}$$

where

$$\begin{aligned}
Q &= \int_{\Gamma_t} N_u^T n N_p \, d\Gamma, \\
S &= \int_{\Omega_f} N_p^T \frac{1}{C^2} N_p \, d\Omega, \\
\widetilde{C} &= \int_{\Gamma_2} N_p^T \frac{1}{C} N_p \, d\Gamma, \\
H &= \int_{\Omega_f} (\nabla N_p)^T \nabla N_p \, d\Omega.
\end{aligned} \tag{13}$$

Free vibration of the coupled system could then be represented by the matrices

$$\begin{bmatrix} M & 0 \\ \rho_f Q^T & S \end{bmatrix} \begin{bmatrix} \ddot{\tilde{u}} \\ \ddot{\tilde{p}} \end{bmatrix} + \begin{bmatrix} K & -Q \\ 0 & H \end{bmatrix} \begin{bmatrix} \tilde{u} \\ \tilde{p} \end{bmatrix} = 0. \tag{14}$$

It should be noted that the force and damping terms present in the original equations (i.e., (11) and (12)) have been ignored in the above equation; the only damping mechanism is, therefore, due to the radiant energy loss. Note that the above equation is not a standard eigenvalue equation (i.e., the type with symmetric matrices); a simple method proposed by Ohayon [1979] could, however, convert it to a standard eigenvalue problem.

Numerical study. This section provides details of the numerical models developed for investigating the vibration response of submerged pipes. The models have been developed in ABAQUS. The eigenvalues of the pipe obtained via the two theories described in the preceding sections are compared. An API-5L X65 steel pipe, commonly used for offshore oil and gas transportation, is considered in this study. The pipe's dimensions and mechanical properties are listed in Table 1. Figure 2 illustrates the cross-section of the submerged pipe modeled via the two approaches. The pipe was modeled with C3D20R elements in ABAQUS (i.e., three-dimensional 20-node reduced integration continuum elements with three translational degrees of freedom per node). Fully restrained boundary conditions (clamped) were assigned to both ends of the pipe by restricting the translational degrees of freedom at the corresponding nodes.

A mesh convergence study, conducted on the pipe, tuned the mesh density to obtain an acceptable convergence level with respect to the computed natural frequencies of interest. Accordingly, a total of 1600 elements connected by 2460 nodes make up the pipe.

elastic modulus (GPa)	206	length (mm)	2000
Poisson's ratio	0.3	outer diameter (mm)	168.3
density (kg/m^3)	7850	wall thickness (mm)	11
yield strength (MPa)	450		

Table 1. Mechanical properties and dimensions of the pipe.
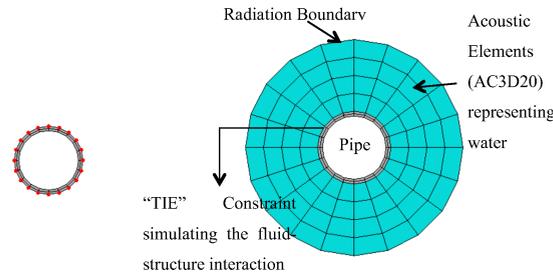
Figure 2. The submerged pipe's models. Left: the added mass approach. Right: the coupled acoustic-structural approach.

As for the first approach, using (7), the total added mass was determined to be 44.36 kg. This mass was evenly distributed on the outer surface of the pipe along its length via lumped masses assigned to the corresponding nodes, as shown in Figure 2, left.

Alternatively, the water surrounding the pipe could be modeled by AC3D20 elements (acoustic three-dimensional 20-node elements with one degree of freedom per node) in ABAQUS. The density and bulk modulus of the fluid must be defined as the material properties for the acoustic element. The corresponding values for water were taken as 997 kg/m^3, and 2.13 GPa, respectively. In addition, the boundary conditions had to be defined on both the acoustic-structural interfaces and infinite boundaries. Hence, a surface-based "TIE" constraint, defined as the interface region, was implemented in the model to simulate the coupling between the pipe and water by correlating the pipe's outer surface nodal displacements to the neighboring water elements' pressure degrees of freedom. Moreover, a radiation boundary was attributed to the exterior boundaries of water to approximate the infinite boundary; this scheme facilitated the transmission of the acoustic waves across the boundaries with little reflection of energy back into the acoustic domain. It should be noted that the reflection from the boundary becomes negligible once the boundary is located far enough from a vibrating structure; Figure 2, right, elucidates these details.

It should also be noted that the extent of the distance that should be included within an acoustic domain in order for the solution to converge efficiently when analyzing various types of problems (i.e., eigenvalue, steady state dynamic, or transient analyses) has been a controversial subject. To overcome this dilemma, the eigenvalues of a submerged pipe in a scaled depth of water were carefully investigated in our study. As such, the performances of the two boundaries as shown in Figure 3 were assessed,
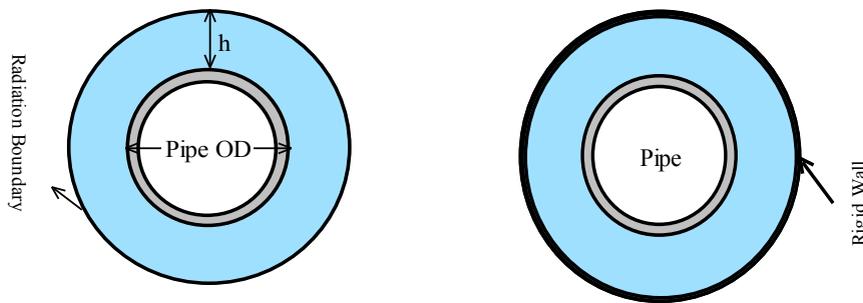

Figure 3. A submerged pipe with radiation (left) and rigid wall (right) boundaries.
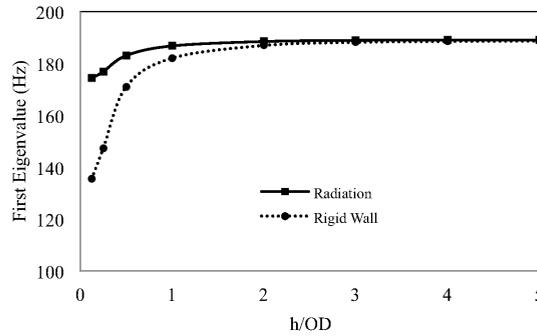
Figure 4. Convergence of the first eigenvalue.

and the results are shown in Figure 4. As can be seen, the first eigenvalue of the pipe converges to a constant value after a certain depth (distance), regardless of the type of the assigned boundary conditions. It is therefore concluded that there would be an effective water level (EWL) beyond which the reflection from the far-field boundary would become negligible. Accordingly, it was determined that modeling the surrounding water to a certain radius (in this case, $h/\text{OD} = 4$) would ensure the convergence of the first six eigenvalues, which are the main focus of this research. It should, however, be highlighted that the EWL may vary significantly depending on the intensity of disturbance caused by the nature of the load(s) within a given analysis (i.e., transient or steady-state dynamic analysis).

Results and discussion. Table 2 compares the eigenvalues of the submerged pipe obtained via the two approaches. The results reveal a noticeable difference in estimation of the third eigenvalue (21% difference) while the variation among the other five eigenvalues is limited to approximately 2%.

The third eigenvalue corresponds to the first torsional mode of the pipe. In this mode, the pipe exchanges almost no energy with the surrounding water. Therefore, it is expected for the torsional modes to yield the same eigenvalues as if the pipe was in the air. The CASA could correctly simulate this condition while, on the other hand, the AMA failed to predict the eigenvalues corresponding to the

Mode	m	n	Pipe in air	Submerged pipe		% difference between
				AMA	CASA	AMA and CASA
1	bending		230.8	187.4	189	0.85
2	bending		580.7	471.5	478.4	1.45
3	torsion		789.9	627.0	789.9	20.60
4	bending		1033.2	838.5	855.4	1.98
5	1	2	1081.1	889.17	907	1.97
6	2	2	1126.5	926.3	947	2.20

m: number of longitudinal half-waves
n: number of circumferential waves [Ustundag 2011]
AMA: added mass approach
CASA: coupled acoustic-structural approach

Table 2. Comparison of the eigenvalues obtained from the AMA and CASA.

torsional modes accurately. A careful examination of the derivation of the added mass term (presented on page 106) reveals that, in that formulation, the velocity potential has been formulated based on the assumption that a submerged pipe would only vibrate in the lateral direction [Blevins 2001]. Hence, the discrepancy associated with this approach is minimized only when the bending modes are dominant, and the contribution of the torsional modes could be ignored.

Based on the above findings, the following recommendation is offered if a successful numerical simulation of a submerged pipeline, in the context of VB-SHM, is desired.

As stated earlier, the AMA has been formulated based upon the consideration of only the lateral vibration of pipes. Therefore, frequency-based VB-SHM approaches that only interrogate the bending eigenvalues of submerged pipes can reliably utilize AMA. However, the accuracy of signal-based (energy-based) VB-SHM approaches could be adversely affected due to the contribution of the torsional, circumferential, and longitudinal mode shapes in the vibration response of a given pipe. For instance, when a submerged pipe is excited by ambient vibration, all mode shapes of the pipe can contribute to its vibration whereas, in the case of an applied impact force perpendicular to the pipe's longitudinal axis, the contribution from the torsional and longitudinal mode shapes becomes relatively negligible in a pipe's vibration response. In addition, the AMA inherently includes other simplification that may cause discrepancies between the results produced by it and those of experiments or real-life situations. The simplifications include the negligence of compressibility and the energy dissipation mechanism induced by the fluid-structure interaction. It should be noted that, in [Razi and Taheri 2014], the authors reported a close agreement between the CASA's prediction of the flexural eigenvalues and the experimentally evaluated ones for a submerged pipe. Consequently, the use of the CASA is recommended when considering the VB-SHM of offshore pipelines.

Effect of operational variability on the accuracy of submerged structures' VB-SHM

In general, any change in the internal or external pressure of a pipe would change its overall stiffness, consequently affecting its vibration response [Rao 2011]. In this case, the equation for free vibration of a pipe is given by

$$\boldsymbol{M}\ddot{\tilde{\boldsymbol{u}}} + \boldsymbol{C}\dot{\tilde{\boldsymbol{u}}} + (\boldsymbol{K}_G + \boldsymbol{K})\tilde{\boldsymbol{u}} = \boldsymbol{0}. \tag{15}$$

The stiffness introduced by the external loads is called the "geometric stiffness", $\boldsymbol{K}_G$ [Cook 1995]. In the case of a submerged pipeline, the internal fluid's pressure or the external hydrostatic pressure would affect the apparent stiffness of the pipe, thereby changing the pipe's eigenvalues and dynamic response.

In VB-SHM techniques, deviations in the eigenvalues or dynamic response of a structure are attributed to the initiation of damage within the structure. Any variation in the geometric stiffness (which in turn alters the eigenvalues) of the structure during a VB-SHM trial could cause false alarms. In the case of a submerged pipeline, such variations could be developed by a sudden drop in the internal fluid's pressure or variation in the depth of submergence (which affects the magnitude of the external hydrostatic pressure).

This section investigates the effect of such operational variability on the eigenvalues and dynamic response of submerged steel and composite pipes. For this purpose, eigenvalues of the pipes when subject to various combinations of internal and external pressures are evaluated. The external pressure on the pipes was varied between 0 to 3 MPa to account for the variable hydrostatic pressure experienced
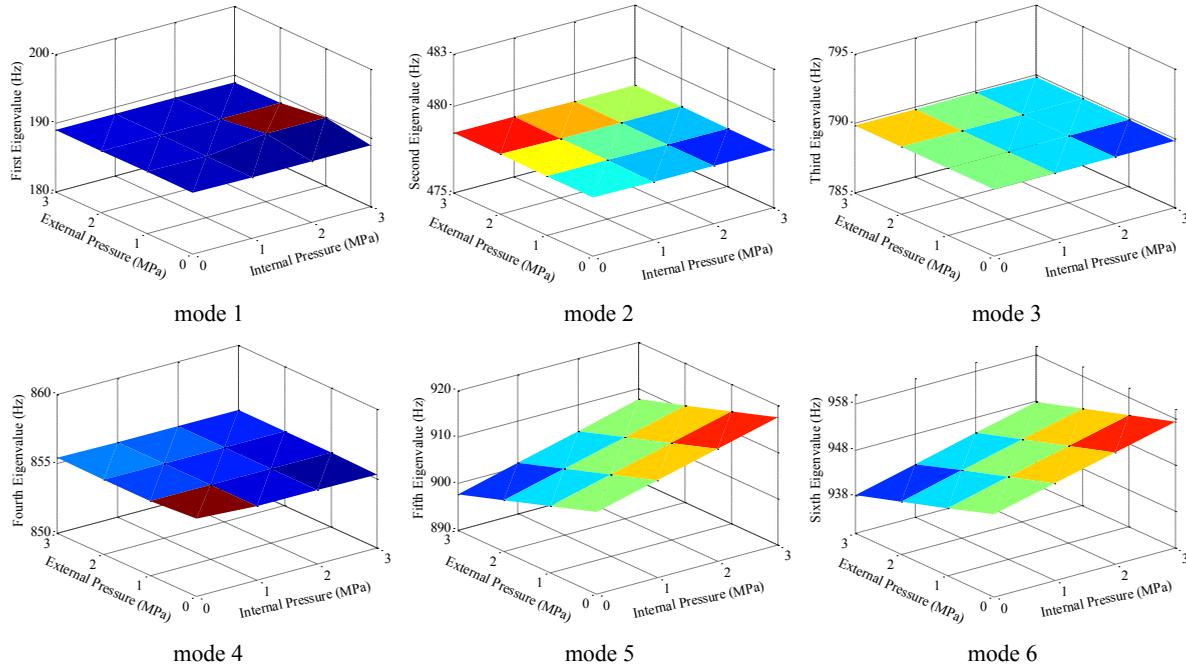
Figure 5. Variation in the eigenvalues of the submerged steel pipe due to varying external and/or internal pressures (buckling pressure (P_{cr}) = 392 MPa): mode 1 (bending), mode 2 (bending), mode 3 (torsional), mode 4 (bending), mode 5 ($m = 1$, $n = 2$), and mode 6 ($m = 2$, $n = 2$), where m is the number of longitudinal half-waves and n is the number of circumferential waves [Ustundag 2011].

by the pipes as the depth of submergence varies between 0 to 300 m. The internal pressure was assumed to vary between 3 to 0 MPa to simulate an internal pressure drop of 3 MPa.

Effect of operational variability on pipes' eigenvalues. The steel pipe described in the previous section was first considered and modeled using the CASA scheme. Figure 5 shows the variation of the submerged pipe's eigenvalues due to the external and/or internal pressures. As can be seen, variations in the eigenvalues corresponding to bending and torsional modes are negligible. However, the mode shapes with longitudinal and circumferential waves (see Figure 6) experienced a maximum of 2% variations in their eigenvalues.

The increase in the external pressure (in the presence of a constant internal pressure) causes a decrease in the eigenvalues of the latter modes while the internal pressure acts in an opposite fashion. The reason is postulated to be because the latter modes include local deformations; therefore, the geometric stiffness, K_G, produced by the internal pressure increases the total stiffness of the pipe, hence providing more resistance against formation of circumferential and longitudinal waves. The external pressure, however, decreases the overall stiffness of the pipe, thereby facilitating the appearance of local deformations. In summary, the geometric stiffness, K_G, developed as a result of the applied external and/or internal pressures would have a greater effect on the overall stiffness of the latter modes (the fifth and sixth modes).
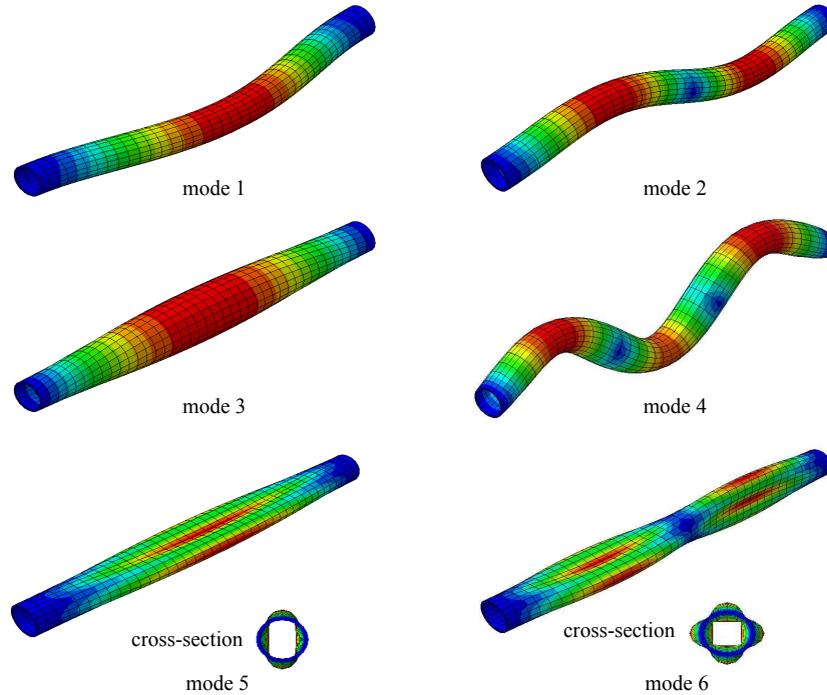
Figure 6. The first six eigenmodes of the steel pipe: mode 1 (bending), mode 2 (bending), mode 3 (torsional), mode 4 (bending), mode 5 ($m = 1$, $n = 2$), and mode 6 ($m = 2$, $n = 2$), where m is the number of longitudinal half-waves and n is the number of circumferential waves [Ustundag 2011].

To examine the effect of the geometric stiffness on pipes' eigenvalues further, two submerged pipes made of fiber-reinforced plastic composites (FRPC) were also considered. One pipe was made of carbon/epoxy and the other was an E-glass epoxy pipe. The lay-up configuration, dimensions, and mechanical properties of the composite pipes are given in Table 3. The pipes were modeled with the S4R element of ABAQUS (i.e., a four-node doubly curved thin or thick shell with finite membrane strains and reduced integration with the hourglass control option). Fully restrained boundary conditions (clamped) were assigned to both ends of the pipe by restraining the translational and rotational degrees of freedom

	Pipe 1	Pipe 2		Carbon/epoxy	E-glass/epoxy
material	carbon/epoxy	E-glass/epoxy	E_{11} (GPa)	138	38.6
length	2	2	E_{22} (GPa)	8.96	8.27
outer diameter	0.1467	0.1545	ν_{12}	0.30	0.26
wall thickness	0.0036	0.0075	G_{12} (GPa)	7.10	4.14
lay-up	$[90/\pm 45]_{3,s}$	$[90/\pm 45]_{5,s}$	ρ (kg/m^3)	1600	1800

Table 3. Dimensions and lay-up of the FRP pipes (m) as well as mechanical properties of composite materials.
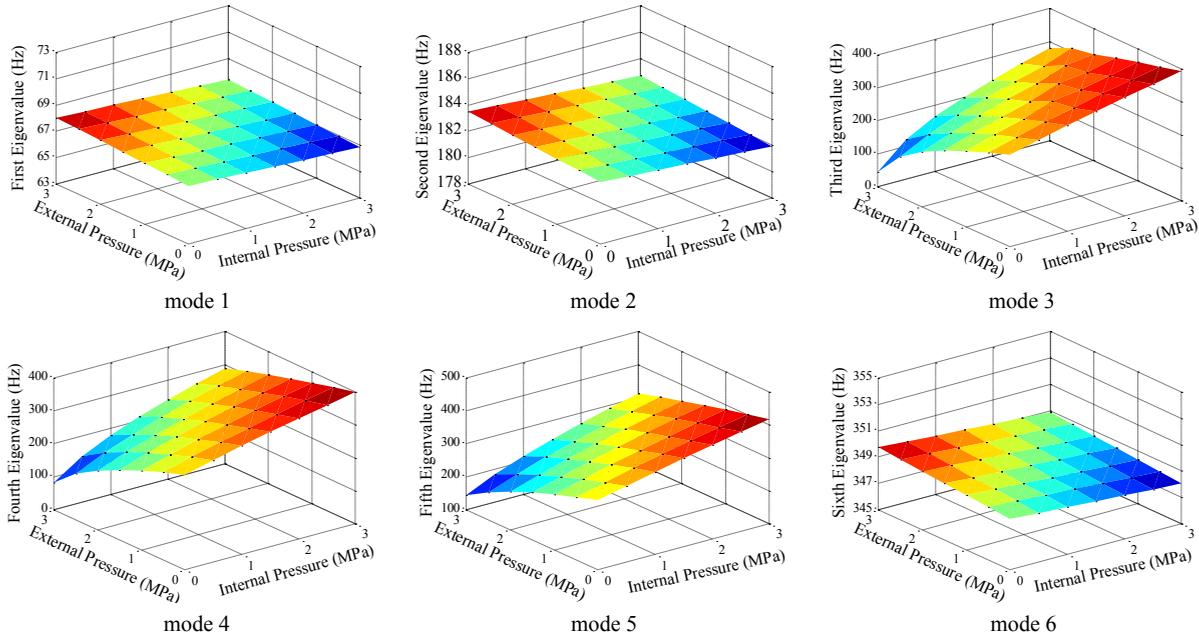
Figure 7. Variation in the eigenvalues of the submerged carbon/epoxy pipe varying due to external and/or internal pressures (design pressure = 15 MPa): mode 1 (bending), mode 2 (bending), mode 3 ($m = 1$, $n = 2$), mode 4 ($m = 2$, $n = 2$), mode 5 ($m = 3$, $n = 2$), and mode 6 (bending), where m is the number of longitudinal half-waves and n is the number of circumferential waves [Ustundag 2011].

of the corresponding nodes. A mesh convergence study was conducted for the pipes based on evaluating the pipes' natural frequencies with the criterion of yielding an acceptable convergence level of 95% with respect to the theoretical values. Accordingly, a total of 800 elements connected by 820 nodes were used to construct the pipe. The surrounding water domain was constructed by 8000 acoustic elements (AC3D8) connected by 9020 nodes.

The lay-up sequence for each pipe was selected such that the pipes could sustain a design pressure of 15 MPa (external/internal) with the same safety factor based on the Hashin damage criterion. Figures 7 and 8 illustrate the variations in the FRPC pipes' eigenvalues against the internal and/or external pressures. As seen, similar to the results obtained from the previous eigenvalue analysis, the bending and torsional modes' eigenvalues of the FRPC pipes experience negligible variations upon applying the net external and internal pressures. The internal pressure generates an effective compressive axial force (see Figure 9), which causes a decrease in the lateral stiffness of the pipe, thereby reducing the eigenvalues corresponding to the bending modes [DNV 2006]. Conversely, the external pressure generates an effective tensile axial force, thereby increasing the eigenvalues corresponding to the bending modes. The other modes' eigenvalues undergo significant variations upon applying the external and/or internal stresses. The trend in variation is also similar to what was observed for the steel pipe. However, the rate of increase/decrease in the eigenvalues is more severe in the case of the FRPC pipes. For instance, the third mode ($m = 1$, $n = 2$) of the FRPC pipe made of carbon/epoxy experiences 84% change in its eigenvalues (i.e., from 280
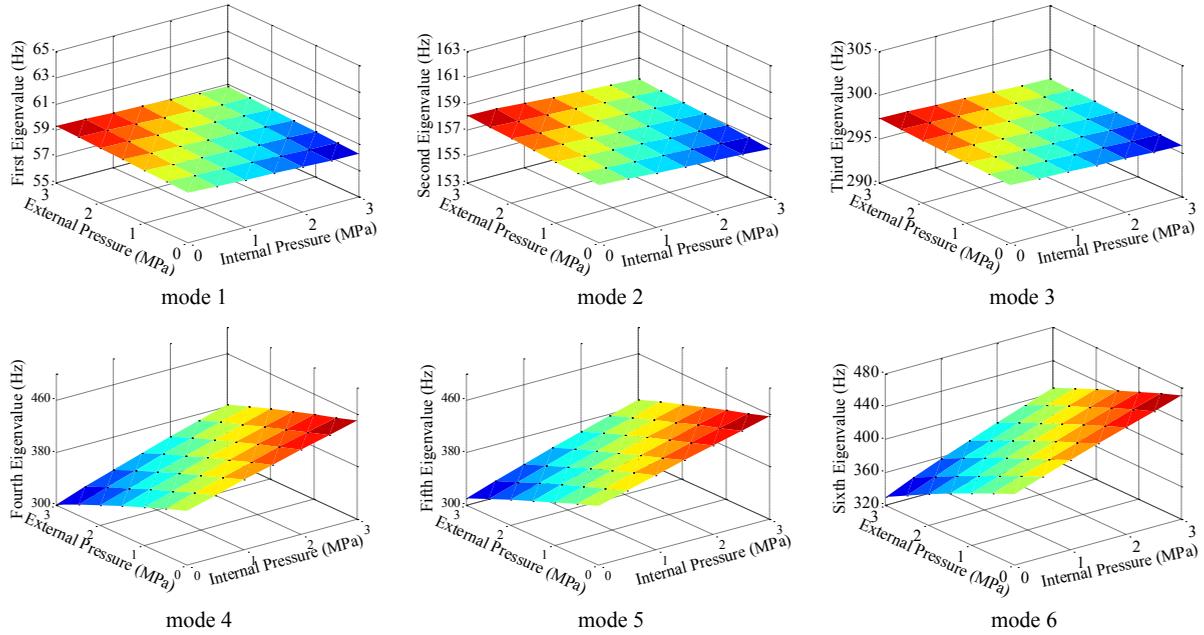
Figure 8. Variation in the eigenvalues of the submerged E-glass/epoxy pipe due to varying external and/or internal pressures (design pressure = 15 MPa): mode 1 (bending), mode 2 (bending), mode 3 (bending), mode 4 ($m = 1$, $n = 2$), mode 5 ($m = 2$, $n = 2$), and mode 6 ($m = 3$, $n = 2$), where m is the number of longitudinal half-waves and n is the number of circumferential waves [Ustundag 2011].

to 44 Hz) as the external pressure increases to 3 MPa (assuming an internal pressure of 0 MPa). For the FRPC pipe made of E-glass/epoxy, however, the variation in the eigenvalues is less severe. For instance, under the same loading condition, the corresponding mode's ($m = 1$, $n = 2$) eigenvalue undergoes 21% reduction (i.e., from 383 Hz to 301 Hz).

These observations imply that the variation in geometric stiffness produced by the presence of the external loads has variably affected the overall stiffness of the FRPC pipes. To explore this phenomenon further, the local stiffness (bending rigidity) of the FRPC pipes was calculated based on the classical laminate theory (CLT) according to the equation [Weisshaar and Foist 1985]

$$\text{EI} = b\left(D_{11} - \frac{D_{12}^2}{D_{22}}\right). \tag{16}$$
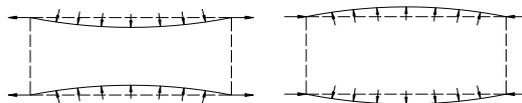

Figure 9. Free body diagrams of the pipe with clamped-clamped boundary conditions. Left: pipe under external pressure. Right: pipe under internal pressure.

FRP carbon/epoxy	98 Pa·m^4
FRP E-glass/epoxy	427 Pa·m^4
Steel pipe	2318 Pa·m^4

Table 4. Bending rigidity (EI) of the FRP and steel pipes.

Table 4 compares the regional bending rigidity of the two FRPC pipes and the steel pipe described in the previous section. The bending rigidity of the pipe made of E-glass/epoxy (wall thickness of 0.0075 m) is approximately four times that of the carbon/epoxy pipe (with wall thickness of 0.0036), which justifies the rate of reduction in the investigated modes' eigenvalue (i.e., 21% in contrast to 84% reduction in the eigenvalue of the mode ($m = 1$, $n = 2$) for the E-glass/epoxy and carbon/epoxy pipes, respectively). On the other hand, the relatively higher stiffness of the steel pipe explains the minor observed variations in the pipe's eigenvalues (i.e., approximately 2% in modes five ($m = 1$, $n = 2$) and six ($m = 2$, $n = 2$)).

The findings from this study can be summarized as follows.

- The accuracy of the frequency-based VB-SHM methods could be adversely affected by the presence of operational variability, depending on the stiffness of the pipe and the severity of variability.

- Accordingly, frequency-based VB-SHM of pipes with high stiffness (e.g., the steel pipe considered in this study) that are subject to operational variability could be successfully accomplished. On the other hand, the VB-SHM of less stiff pipes (such as the FRPC pipes considered in this study) should be conducted cautiously and diligently since their eigenvalues happen to be quite sensitive to the operational variation.

Effect of operational variability on the transient dynamic response of pipelines. The transient dynamic responses of pipes would also be affected as a result of a change in their stiffness. For instance, the same carbon/epoxy pipe examined earlier is subjected to an impact load in the form exhibited in Figure 10 under the conditions described in Figure 11. The pipe was impacted at 0.5 m from its left end, and the transient responses (i.e., acceleration (a_y), velocity (v_y), and displacement (d_y) time-histories) of a point along the pipe, located 0.6 m from the left end, were collected (see Figure 10). As can be seen in Figure 11, the existence of the external pressure (3 MPa) on the pipe tangibly alters the transient responses of the pipe, both in terms of the amplitude and energy.
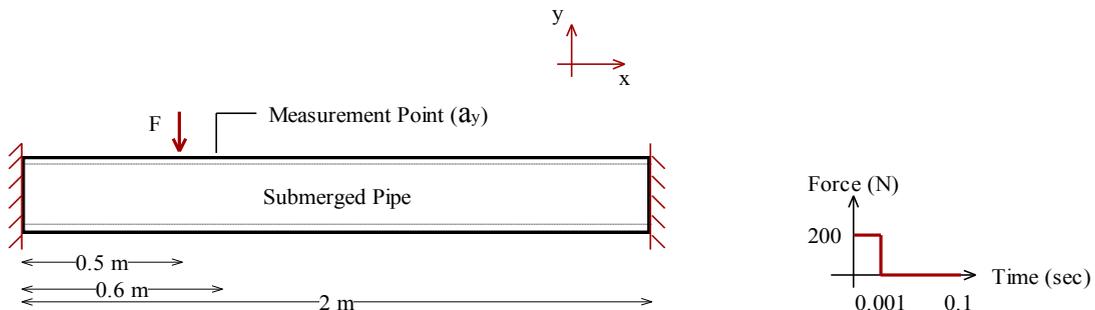

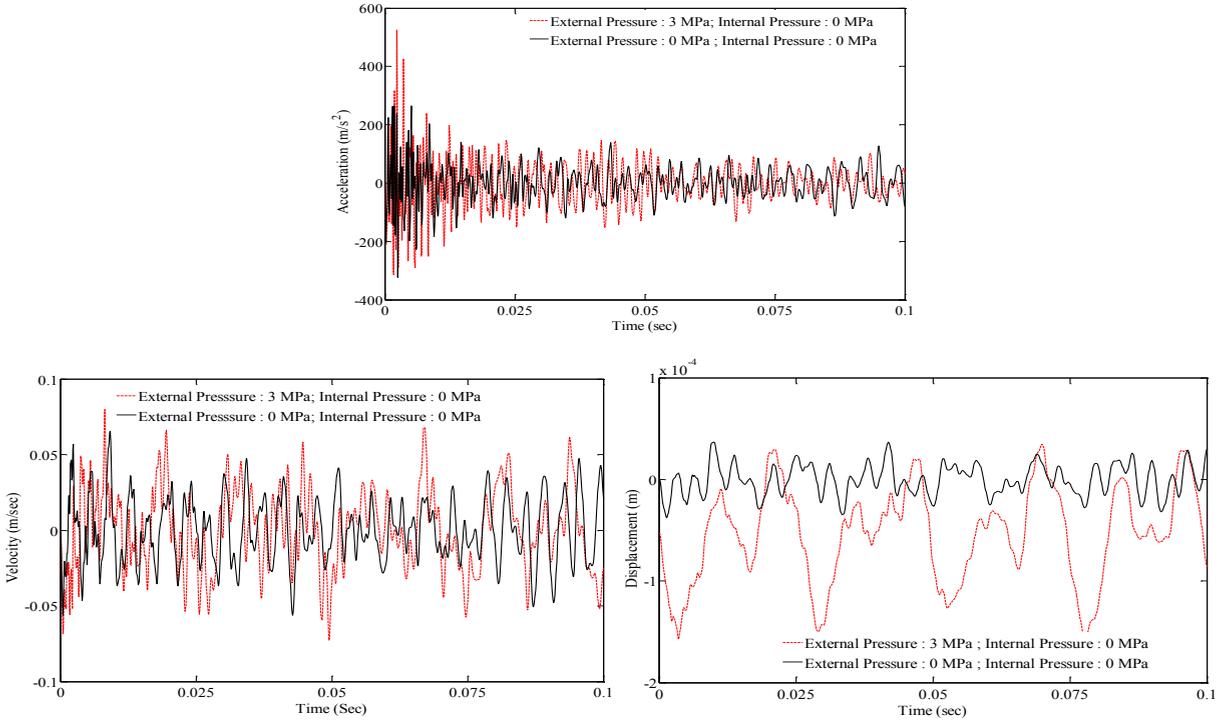**Figure 10.** Left: schematic of the submerged pipe. Right: the transient applied load.

Figure 11. Acceleration (top), velocity (bottom left), and displacement (bottom right) time-histories of the selected point on the FRP pipe (made of carbon/epoxy) due to an impact load.

Several VB-SHM methods' damage-sensitive features are based on the time-domain vibration response of the system being monitored [Peng et al. 2012; Bao et al. 2013; 2011; Rezaei and Taheri 2010]. As demonstrated earlier, the vibration response of pipelines could be significantly affected as a result of operational variability (i.e., variation in either the internal fluid's pressure or external hydrostatic pressure or both). Neglecting such influential parameters could significantly affect the accuracy of VB-SHM methods. Therefore, since the SHM of interest to us is a coupled signal and vibration-based approach, it would be instructive to evaluate the degree of sensitivity of the methodology to such operational variability.

The VB-SHM technique that has been developed in our research group [Rezaei and Taheri 2010; Razi et al. 2013] is based on the examination of the energy of the first intrinsic mode function (IMF) of the time-domain vibration response of a given structure. This quantity is used as a damage-sensitive feature and is mathematically represented by the equation

$$E = \int_0^{t_0} (\text{IMF } 1)^2 \, dt, \tag{17}$$

where t_0 is the signal duration. The IMFs of a typical vibration response can be obtained by applying the empirical mode decomposition (EMD), a signal-processing technique, to the time-domain vibration response of the system. Evaluation of the above term during a structures' service life enables detection
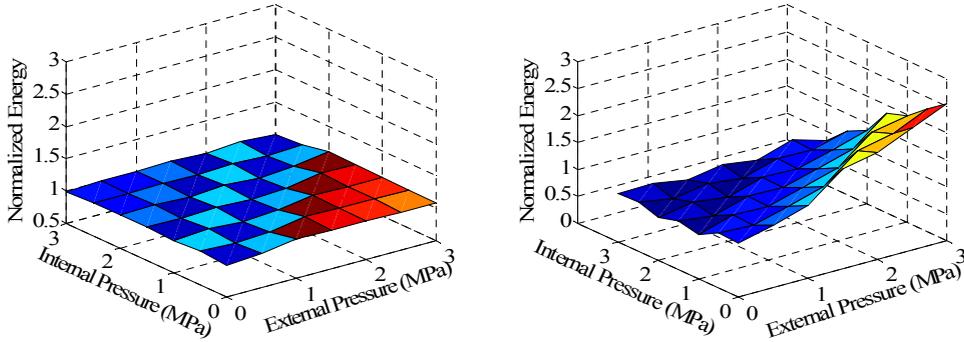
Figure 12. Variation in the energy of the acceleration time-history's first IMF as a function of external and internal pressures. Left: steel pipe. Right: FRPC (carbon/epoxy).

of damage within the structures by using the damage index formulation

$$\text{EMD\_EDI} = \left| \frac{E_{\text{healthy}} - E_{\text{damaged}}}{E_{\text{healthy}}} \right| \times 100, \tag{18}$$

where E_{healthy} and E_{damaged} correspond to the energy of the first IMF of the vibration response evaluated at the structure's healthy and damaged states. An index larger than 0 would indicate the presence of damage. As noted, however, the energy term, E, could be affected by the presence of operational variability, some of which was explained earlier, and the consequence could be false alarms in detection of damage.

To investigate the sensitivity of the EMD_EDI to the operational variability, the time-histories of the vibration responses of the FRPC and steel pipes due to an impact load (see Figure 10) were considered.

Figure 12 illustrates the variation of the energy term, E, for the steel pipe and the pipe with the lowest bending rigidity, namely FRPC (glass/epoxy), as a function of the applied external and internal pressures. Note that the values are normalized with respect to the energy of the pipes in their unpressurized state (i.e., $P_{\text{Internal}} = P_{\text{External}} = 0 \, \text{MPa}$).

The results indicate that the energy term corresponding to the steel pipe undergoes a very minor change (a maximum of 10%) over the entire pressure domain. In contrast, the FRPC pipe's vibration response shows considerable sensitivity to the variation in applied pressures (by as much as 150%). The sensitivity is believed to be because of the steel pipe's flexural stiffness, which was notably higher than the FRPC pipes' stiffness (see Table 4). As a result, the contribution of the geometric stiffness (K_G) to total stiffness was negligible in the case of the steel pipe. According to (18), the imposed variation in the energy of the pipes due to variation in the applied pressures could lead to false alarms in prediction of potential damages.

The authors [Razi and Taheri 2014] reported the result of a damage detection trial conducted on a submerged pipe based on the evaluation of the energy term described above (i.e., E). They considered SHM of a propagating notch in the girth-weld of two mating pipes. The notably large values of damage index reported in this study (i.e., from 25%, corresponding to the notch at 1 mm deep, up to 150% when the notch depth propagated to 4 mm) suggests that the result of damage detection on the steel pipe would remain insensitive to the disturbance caused by the variation in the external or internal pressure

considered in this study. On the other hand, SHM of pipes with relatively low bending rigidity (e.g., the carbon/epoxy pipe examined here) could lead to false alarms in the presence of such disturbance.

The results from this part of the study can be summarized as follows.

- When investigating the health of an offshore pipeline, the integrity of the energy-based (or signal-based) VB-SHM methodologies could be greatly affected depending by the pipe's stiffness and the extent of variation in the external and internal pressures that the pipe would experience during a VB-SHM trial.

- The VB-SHM of stiff submerged pipes (e.g., the steel pipe considered in this study) using the EMD_EDI method can be accomplished with a good level of confidence and accuracy. This accuracy would be met, provided the pipe experiences a sudden drop in its internal pressure (up to 3 MPa according to this study's result) or when the depth of submergence changes within 300 m (i.e., 3 MPa change in the external pressure). The results of the EMD_EDI method applied to less stiff pipes (i.e., the FRPC composite pipes considered here) indicate that SHM of such pipes would be a challenging task. This is mainly due to the fact that their vibration response could undergo a significant change under imposed operational variability.

Concluding remarks

The performance and accuracy of the two widely used approaches for modeling the dynamic response of submerged structures (namely, the "added mass" and "coupled acoustic-structural" approaches) in the context of VB-SHM were investigated. The investigation included the evaluation of the eigenvalues of an offshore pipeline modeled by the two approaches. The differences were limited to below 2% in the lateral modes whereas for the torsional mode the differences approached 20%. The large discrepancy was attributed to the restrictive assumption involved in the formulation of the "added mass" approach. It was therefore recommended to adopt the coupled acoustic-structural approach to conduct successful VB-SHM of submerged structures.

Subsequently, the effect of operational variability on the accuracy of a VB-SHM of offshore pipelines was studied. Such operational variability could rise due to the change in the pressure of the fluid with which the pipe is pressurized or the change in the external hydrostatic pressure upon submergence of the pipe in various depths. For this purpose, vibration response of a steel and two FRPC composite pipes was examined against incremental variations in the internal and external pressures. Our findings can be summarized as follows.

- The accuracy of VB-SHM of pipes could be adversely affected by operational variability. The adverse impact would be a function of the stiffness of the pipe.

- Accordingly, it was determined that VB-SHM of the steel pipe considered in this study could be successfully conducted under the examined operational variability. On the other hand, the VB-SHM trial should be conducted with diligence for less stiff pipes such as the FRPC composite pipes considered in this study as their vibration response showed notable sensitivity to the operational variability.

List of symbols

b	width		N_u	shape functions for displacement
C	speed of sound in the medium		N_p	shape functions for acoustic pressure
$\boldsymbol{C}$	damping matrix		p_s	static pressure
$\widetilde{\boldsymbol{C}}$	damping matrix for fluid		p	dynamic/acoustic pressure
D_{ij}	bending stiffness elements		$\tilde{\boldsymbol{p}}$	acoustic pressure vector
E_{ij}	elastic moduli		$\boldsymbol{Q}$	coupling matrix
EI	bending rigidity		r	radius
$\boldsymbol{F}$	force vector		$\boldsymbol{S}$	mass matrix for fluid
g	acceleration due to gravity		U	velocity in lateral direction
G_{ij}	shear moduli		$\boldsymbol{u}$	displacement vector
h	height of the fluid		$\tilde{\boldsymbol{u}}$	nodal displacements vector
H	stiffness matrix for fluid		V	velocity
OD	outer diameter		$X(t)$	displacement in x-direction
K	stiffness per unit length		Ω_f	fluid domain
$\boldsymbol{K}_G$	geometric stiffness matrix		Γ_i	boundary domain
M	mass per unit length		ρ_f	fluid density
$\boldsymbol{M}$	mass matrix		ϕ	velocity potential
$\boldsymbol{n}$	unit normal vector		ν_{ij}	Poisson's ratio

Acknowledgements

References

[Bao et al. 2011] C.-X. Bao, H. Hao, and Z.-X. Li, "Vibration-based damage detection of pipeline system by HHT method", *Applied Mechanics and Materials* **99–100** (2011), 1067–1072.

[Bao et al. 2013] C.-X. Bao, H. Hao, and Z.-X. Li, "Vibration-based structural health monitoring of offshore pipelines: numerical and experimental study", *Structural Control and Health Monitoring* **20**:5 (2013), 769–788.

[Blevins 2001] R. D. Blevins, *Flow-induced vibration*, 2nd ed., Krieger, Malabar, FL, 2001.

[Cengel and Cimbala 2006] Y. A. Cengel and J. M. Cimbala, *Fluid mechanics: fundamentals and applications*, McGraw-Hill, New York, 2006.

[Chen et al. 2010] J. Chen, Z. Su, and L. Cheng, "Identification of corrosion damage in submerged structures using fundamental anti-symmetric Lamb waves", *Smart Materials and Structures* **19**:1 (2010), 015004.

[Cook 1995] R. D. Cook, *Finite element modeling for stress analysis*, Wiley, New York, 1995.

[DNV 2006] "Free spanning pipelines", recommended practice DNV-RP-F105, Det Norske Veritas, 2006, Available at http://exchange.dnv.com/publishing/codes/docs/2006-02/RP-F105.pdf.

[Kramer et al. 2013] M. R. Kramer, Z. Liu, and Y. L. Young, "Free vibration of cantilevered composite plates in air and in water", *Composite Structures* **95** (2013), 254–263.

[Na and Kundu 2002] W.-B. Na and T. Kundu, "Underwater pipeline inspection using guided waves", *Journal of Pressure Vessel Technology* **124**:2 (2002), 196–200.

[Ohayon 1979] R. Ohayon, "Symmetric variational formulation of harmonic vibrations problem by coupling primal and dual principles. Application to fluid-structure coupled systems", *La Recherche Aérospatiale* **3** (1979), 207–211.

[Peng and Hao 2012] X.-L. Peng and H. Hao, "A numerical study of damage detection of underwater pipeline using vibration-based method", *International Journal of Structural Stability and Dynamics* **12**:3 (2012), 1250021.

[Peng et al. 2012] X.-L. Peng, H. Hao, and Z.-X. Li, "Application of wavelet packet transform in subsea pipeline bedding condition assessment", *Engineering Structures* **39** (2012), 50–65.

[Rao 2011] S. S. Rao, *Mechanical vibrations*, 5th ed., Prentice Hall, Upper Saddle River, NJ, 2011.

[Razi and Taheri 2014] P. Razi and F. Taheri, "A vibration-based strategy for health monitoring of offshore pipelines' girth-welds", *Sensors* **14**:9 (2014), 17174–17191.

[Razi et al. 2013] P. Razi, R. A. Esmaeel, and F. Taheri, "Improvement of a vibration-based damage detection approach for health monitoring of bolted flange joints in pipelines", *Structural Health Monitoring* **12**:3 (2013), 207–224.

[Rezaei and Taheri 2010] D. Rezaei and F. Taheri, "Health monitoring of pipeline girth weld using empirical mode decomposition", *Smart Materials and Structures* **19**:5 (2010), 055016.

[Rizzo et al. 2010] P. Rizzo, J.-G. Han, and X.-L. Ni, "Structural health monitoring of immersed structures by means of guided ultrasonic waves", *Journal of Intelligent Material Systems and Structures* **21**:14 (2010), 1397–1407.

[Ross et al. 2007] C. T. F. Ross, P. Köster, A. P. F. Little, and G. Tewkesbury, "Vibration of a thin-walled prolate dome under external water pressure", *Ocean Engineering* **34**:3–4 (2007), 560–575.

[Ustundag 2011] B. Ustundag, *On the free vibration behavior of cylindrical shell structures*, master's thesis, Massachusetts Institute of Technology, Cambridge, MA, 2011, Available at http://hdl.handle.net/1721.1/67717.

[Weisshaar and Foist 1985] T. A. Weisshaar and B. L. Foist, "Vibration tailoring of advanced composite lifting surfaces", *Journal of Aircraft* **22**:2 (1985), 141–147.

[Zeinoddini et al. 2012] M. Zeinoddini, G. A. R. Parke, and S. M. Sadrossadat, "Free-spanning submarine pipeline response to severe ground excitations: water-pipeline interactions", *Journal of Pipeline Systems Engineering and Practice* **3**:4 (2012), 135–149.

[Zhu et al. 2008] X. Q. Zhu, H. Hao, and X.-L. Peng, "Dynamic assessment of underwater pipeline systems using statistical model updating", *International Journal of Structural Stability and Dynamics* **8**:2 (2008), 271–297.

[Zienkiewicz et al. 2005] O. C. Zienkiewicz, R. L. Taylor, and J. Z. Zhu, *The finite element method: its basis and fundamentals*, 6th ed., Butterworth–Heinemann, Oxford, 2005.

[Zou et al. 2005] G. P. Zou, N. Cheraghi, and F. Taheri, "Fluid-induced vibration of composite natural gas pipelines", *International Journal of Solids and Structures* **42**:3–4 (2005), 1253–1268.

PEJMAN RAZI: Pejman.razi@dal.ca
Department of Civil and Resource Engineering, Dalhousie University, 1360 Barrington Street, Halifax, NS B3H 4R2, Canada

FARID TAHERI: farid.taheri@dal.ca
Department of Civil and Resource Engineering, Dalhousie University, 1360 Barrington Street, Halifax, NS B3H 4R2, Canada

JOURNAL OF MECHANICS OF MATERIALS AND STRUCTURES

msp.org/jomms

Founded by Charles R. Steele and Marie-Louise Steele

Cover photo: Ev Shafrir